Available online at www.sciencedirect.com
ScienceDirect
Journal of Power Sources 174 (2007) 321–327
JOURNAL OF POWER SOURCES
www.elsevier.com/locate/jpowsour

The role of the interface of tin electrodes in lithium cells: An impedance study

J. Hassoun *, P. Reale, S. Panero

Department of Chemistry, University of Rome "La Sapienza", 00185 Rome, Italy

Received 27 July 2007; received in revised form 10 September 2007; accepted 10 September 2007
Available online 21 September 2007

Abstract

In this work we investigate by impedance spectroscopy the characteristics of a film formed on the surface of Sn electrodes when cycled in a lithium cell. We show that this film is formed by electrolyte decomposition catalyzed by the tin surface and that its characteristics depend upon cycling rate as reported in the literature. By the infrared analysis we study the chemical characteristic of mentioned film. By reporting the cycling response of a complete lithium-ion battery using a Sn anode coupled with a $LiNi_{0.5}Mn_{1.5}O_4$ cathode, we show that the interfacial film may indeed influence the response of the batteries using conventional, tin-based anodes.

Keywords: Tin electrodes; Interface; Impedance spectroscopy; Lithium-ion battery

1. Introduction

In a series of papers, Dahn and co-workers [1–3] demonstrated the occurrence of one anomalous irreversible plateau on the initial discharge curve of a Sn electrode when cycled in a lithium cell. The extent of this plateau, which evolves around 1.5 V versus Li, depends on the cycling rate, being longer as the rate decreases. This film was attributed to the decomposition of the electrolyte, catalyzed by the tin surface, which in turn gives rise to the formation of a passivation film on the surface of the electrode.

Considering the relevance of Sn electrodes in the advanced lithium battery science and technology [4], it has appeared to us of interest to extend the investigation of this anomalous surface film and of the processes which cause its formation. It is in fact expected that the phenomena may influence the response of batteries using tin as anode material, as indeed demonstrated in this work.

2. Experimental

Tin samples were obtained by electrodeposition on a copper foil in a two-electrode glass cell, using a current density of 6 mA cm^{-2} for 5 min at room temperature. An aqueous solution, formed by KCl 0.15 M, $SnCl_2$ 0.175 M, $K_4P_2O_7$ 0.5 M, glycine 0.125 M and NH_4OH 5 ml l^{-1}, was used as the electrolyte and a Pt foil as the counter electrode [5]. The electroplating current and time conditions were monitored using a Maccor Series 4000 Battery Test System.

The structure of the samples was investigated by XRD, using a Rigaku Miniflex X-ray diffractometer and their morphology by scanning electron microscopy, SEM, using SEM Leo EVO 40.

The electrochemical response of the tin electrode samples was studied in a cell based on the following configuration: (i) a Sn working electrode with a diameter of 1.0 cm, (ii) a 1 M $LiPF_6$ in ethylene carbonate-dimethyl carbonate, EC:DMC 1:1 (Merck Battery Grade) electrolyte solution soaked on a Whatman™ separator and (iii) a lithium metal foil counter electrode. An additional lithium foil reference electrode was used for the impedance spectroscopy measurements. The cells were cycled at 1 C and 0.1 C (around 1.2 A cm^{-2} g^{-1} and 0.12 A cm^{-2} g^{-1},

* Corresponding author. Tel.: +39 06 49913530; fax: +39 06 491769.
E-mail address: jusef.hassoun@uniroma1.it (J. Hassoun).

0378-7753/$ – see front matter © 2007 Elsevier B.V. All rights reserved.
doi:10.1016/j.jpowsour.2007.09.046

respectively versus Sn active mass) and within a 0.01–1.5 V voltage limit, using a Maccor Series 4000 Battery Test System as the controlling instrument.

The infrared spectrum of the film, formed on the Sn electrode after the 1st galvanostatic cycle at C/10 rate, was performed, after the electrode drying at room temperature under vacuum for 1 h, using a UNICAM Mattson 5000 FTIR spectrometer in the attenuated total reflection (ATR) mode equipped with a Specac golden gate using a single reflection diamond crystal. The spectra are the result of 50 scans with a resolution of 4 cm^{-1}.

The impedance spectroscopy analysis was carried out by applying a 10 mV amplitude signal in the 100 kHz to 0.005 Hz frequency range using a frequency response analyzer (FRA) Schlumberger Solartron model 1260 coupled with EG&G Princeton Applied Research model 362 potentiostat.

The lithium-ion cells were formed by coupling the selected Sn sample anodes with a $LiNi_{0.5}Mn_{1.5}O_4$ cathode [6] in a 1 M $LiPF_6$ EC:DMC 1:1 electrolyte solution. The cathode was prepared as a thin film on an aluminium substrate by doctor-blade deposition of a slurry composed of 80% $LiNi_{0.5}Mn_{1.5}O_4$ (active material), 10% PVdF 6020, Solvay Solef (binder) and 10% SP carbon (electronic support). The cell was cycled within a 2.5–5 V voltage range and at various rates (1 C corresponding to 0.2 Ag^{-1} cm^{-2}) using a Maccor Series 4000 Battery Test System as the controlling instrument.

3. Results and discussion

This work is addressed to the investigation of an unexpected irreversible plateau which occurs on the initial discharge curve of conventional, pure tin electrodes when cycled at low rates in a lithium cell. This plateau is associated with the decomposition of the electrolyte with the formation of a film on the electrode surface [1–3]. In this work, we analyse this anomalous phenomenon with the main objective of determining its influence on the response of lithium batteries using tin-based anodes. For this study we have selected a Sn electrode prepared by electrodeposition on a copper substrate [5].

The SEM image illustrated by Fig. 1 reveals that the electrode has a porous, pillar-like morphology with a large surface development.

Fig. 2 shows the XRD patterns of a typical Sn electrode sample. Only the peaks of the support and those of metallic tin are revealed, which confirms the purity of the sample.

The Sn electrodes prepared in this work were tested in half lithium-ion cells using a lithium metal counter electrode and a EC:DMC 1:1, 1 M $LiPF_6$ electrolyte. The overall electrochemical process of these cells is expected to be the alloying–dealloying of lithium in tin:

$$4.4Li + Sn \leftrightarrows Li_{4.4}Sn \quad (1)$$

In detail, the process is represented by the following progression of reactions:

$$5Sn + 2Li^+ + 2e^- \leftrightarrows Li_2Sn_5 \quad (2)$$

$$Li_2Sn_5 + 3Li^+ + 3e^- \leftrightarrows 5LiSn \quad (3)$$

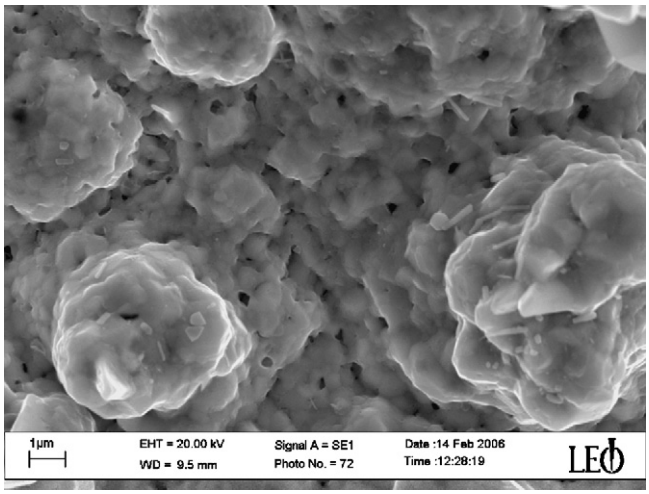

Fig. 1. SEM image of a typical sample of the Sn electrodes prepared in this work.

$$3LiSn + 4Li^+ + 4e^- \leftrightarrows Li_7Sn_3 \quad (4)$$

$$2Li_7Sn_3 + Li^+ + e^- \leftrightarrows 3Li_5Sn_2 \quad (5)$$

$$5Li_5Sn_2 + Li^+ + e^- \leftrightarrows 2Li_{13}Sn_5 \quad (6)$$

$$2Li_{13}Sn_5 + 9Li^+ + 9e^- \leftrightarrows 5Li_7Sn_2 \quad (7)$$

$$5Li_7Sn_2 + 9Li^+ + 9e^- \leftrightarrows 2Li_{22}Sn_5 \quad (8)$$

The lithium cells were cycled at different rates, i.e., one at C/10 and the other at 1 C. Fig. 3A shows the voltage profile of the first cycle of the cell cycled at the low C/10 rate. A wide voltage plateau, placed near 1.5 V versus Li, is clearly visible. This plateau cannot be associated to the main electrochemical process (1), but rather to electrolyte decomposition. In fact, the plateau is not reproducible and its extension decreases passing from 1st to following cycles, see Fig. 3B.

Fig. 4 illustrates the response of the second cell cycled at a ten times higher rate, i.e. at 1 C. The figure compares the voltage profile of the first cycle (Fig. 4A) with that of the following cycles (Fig. 4B). The extension of the anomalous plateau is here consistently reduced and the voltage rapidly assumes the signa-

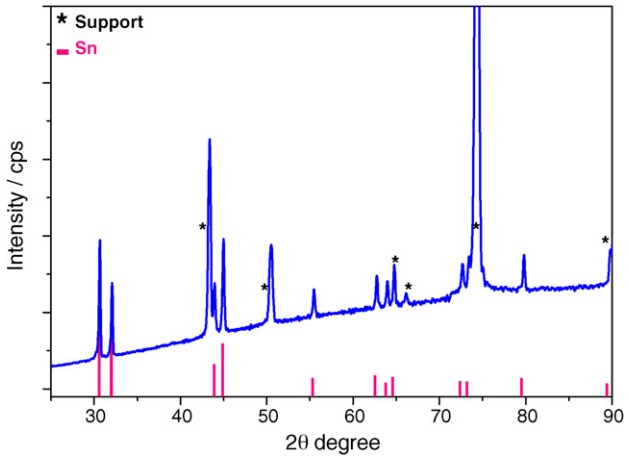

Fig. 2. XRD patterns of a Sn electrode prepared in this work.

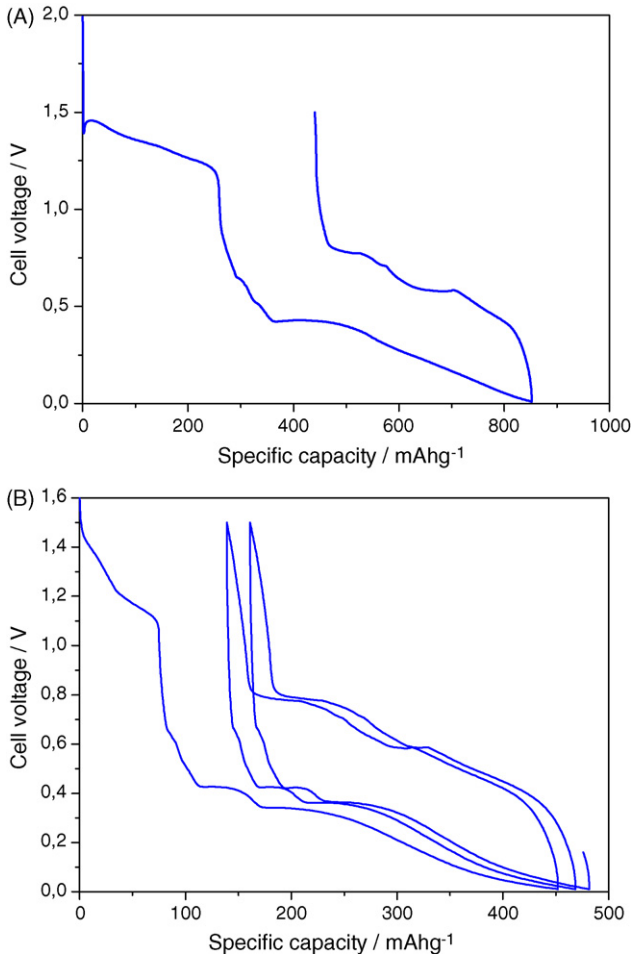

Fig. 3. Voltage vs. specific capacity profiles during the first discharge (Li alloying in Sn)–charge (Li dealloying from Sn) cycle (A) and during the subsequent cycles (B) of a Sn/EC:DMC 1:1 $LiPF_6$/Li cell. Charge current density: 0.126 A cm^{-2} g^{-1}, C/10 rate. Voltage limits: 0.01–1.5 V. Room temperature.

ture expected by process (1), confirming that the occurrence of the plateau is controlled by the rate.

The critical role of the cycling rate is also confirmed by Fig. 5 which compares the specific capacity versus cycle number for two Li–Sn cells cycled under the two different regimes, i.e. at C/10 and at 1 C, respectively. As expected, the cycled reversible capacity is higher for the cell cycled at the higher rate. Indeed, considering that the low rate favours the formation of the film, the decay in capacity observed for the cell cycled at C/10 is not surprising. Quite likely, the irreversible process at 1.5 V, which leads to the formation of the surface film, compromises part of the active material on the electrode surface, this inducing consistent volume variations with consequent cracking upon cycling [5,7].

Considering that the 1.5 V plateau is associated with a passivation film deposited on the surface of the tin electrode [2], a FT-IR analysis was performed using a Sn electrode after the 1st galvanostatic cycle at C/10 rate. The IR spectrum, reported in Fig. 6, confirms the presence of a composite film on the tin surface consisting of an organic part ($ROCO_2Li$) and an inorganic salt (Li_2CO_3) as the electrolyte decomposition products, as well as residual crystallized solvent (EC). Similar results have

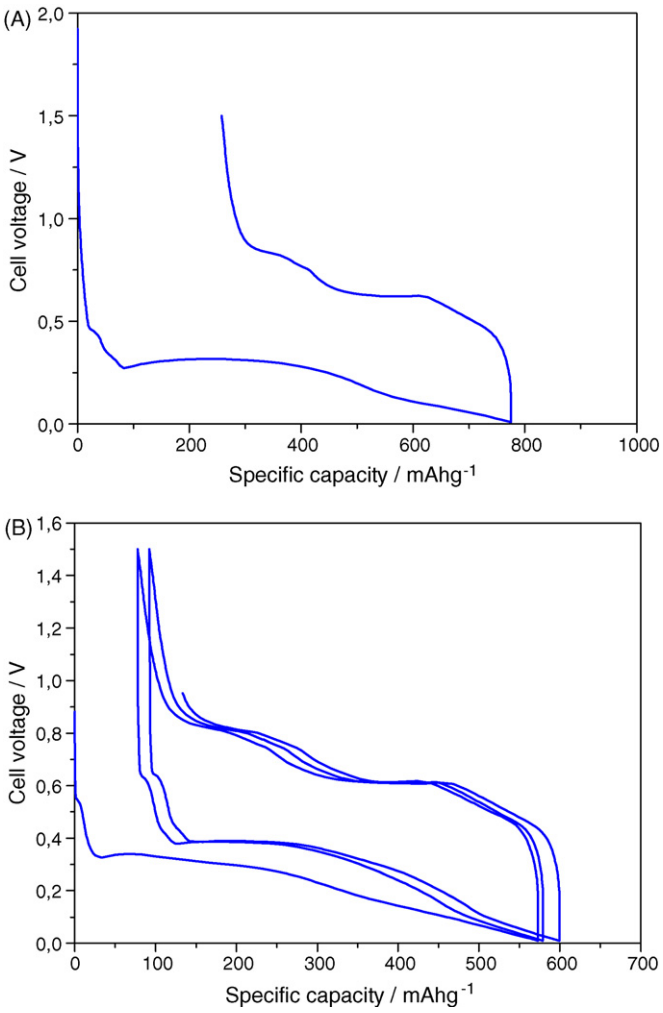

Fig. 4. Voltage vs. specific capacity profiles during the first discharge charge cycle (A) and during the subsequent cycles (B) of a Sn/EC:DMC 1:1 $LiPF_6$/Li cell. Charge–discharge current density 1.26 A cm^{-2} g^{-1}, 1 C rate. Voltage limits: 0.01–1.5 V. Room temperature.

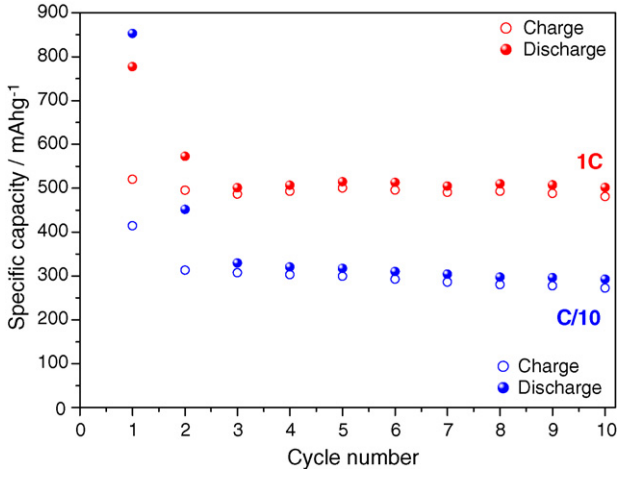

Fig. 5. Specific capacity vs. cycle number for Sn/EC:DMC 1:1 $LiPF_6$/Li cells cycled under two different current regimes, i.e., at C/10 rate and at 1 C rate. Charge–discharge current density at: 0.126 A cm^{-2} g^{-1} and 1.26 A cm^{-2} g^{-1}, respectively. Voltage limits: 0.01–1.5 V. Room temperature.

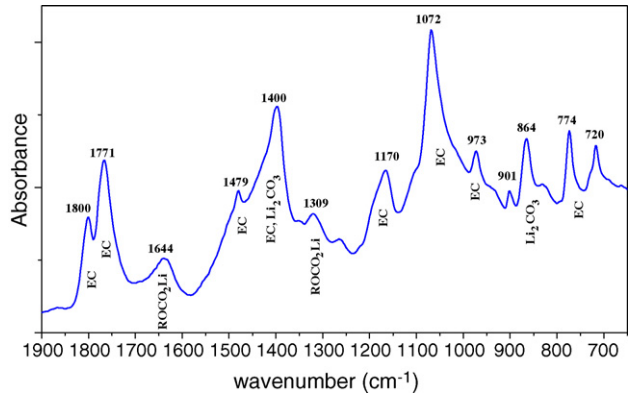

Fig. 6. IR spectrum of a Sn electrode after the 1st galvanostatic cycle at C/10 rate.

been also reported by Geniès et al. [8] studying the passivation phenomena on a graphitized mesocarbon fibers. Moreover, alkyl carbonates products have been also revealed on lithium surface, which tend to dominate the build-up of the Li-solution interfaces [9].

The formation of this film may have important practical reflections, e.g., in affecting the performance of lithium batteries using a tin electrode. Thus, it has appeared to us of interest to further investigate its characteristics. In this respect, we have undertaken an impedance spectroscopy analysis of the two cells considered in this work. The choice is motivated by the potentiality of the technique in defining interfacial phenomena, as those associated to the formation of electrode surface films. Thus, impedance spectroscopy appears particular useful for shedding more light on the phenomena occurring at the tin interface under the conditions examined in this work.

Fig. 7A compares the impedance response after the first discharge cycles of the two cells considered in this work and differing by the cycling rate, i.e. one cycled at C/10 and the other at 1 C. Similarly, Fig. 7B compares the impedance response of the same cells cycled at different rates; however, in this case the impedance test was run after the 10th cycle. We see that in both cases the response may qualitatively be described in terms of two semicircles, related to surface films and charge transfer kinetics, respectively, followed by a low frequency inclined line, related to cell geometric capacitance [10]. However, while the trend in the low frequency region is similar for both cells, a significant difference is observed in the high frequency region.

The impedance responses were analysed using a common approach followed studying similar phenomena, i.e. by defining an equivalent circuit taking into account all possible contributes to the impedance of the tested cells [10]. Accordingly, using as circuital elements resistances R and a constant-phase elements (CPE) Q in the place of pure capacitance, the general equivalent circuit which may adequately represent the response of the cell cycled at 1 C rate, has to take into account the electrolyte contribution to the total resistance (R_e), the contribution of the surface film (R_f, Q_f in parallel), the charge transference contribution (R_{ct}, Q_{ct} in parallel) and, finally, the cell contribution which takes into account the cell geometric capacitance (Q_g), see Fig. 8A.

To represent the response of the cell cycled at C/10, an equivalent circuit similar to the previous one, except for the presence of an additional contribution (R_{f2}, Q_{f2}) in the medium-high frequency associated to a more complex nature of the surface film, was used, see Fig. 8B. The validity of the chosen circuits was confirmed by fitting the impedance response using a Non-Linear Least-Square (NLLSQ) fit software developed by Boukamp [11,12]. The matching with the experimental data is quite good, with a Chi-square factor of the order of 10^{-4} which is considered an acceptable pre-requisite to the validity of the proposed model.

Fig. 9 reports the overlapping of the impedance responses with the approximate representation of the correspondent circuital elements for the cell cycled at 1 C (A) and at C/10 (B) after the first cycle.

Table 1 lists the impedance parameters obtained by fitting the impedance spectra related to the cell cycled at 1 C rate and Table 2 those related to the cell cycled at C/10. The impedance tests have been repeated on several cells, cycled either at 1 C and at C/10, obtaining data which, within the experimental error limits, are consistent to those above reported in the tables.

These data show that to the very high frequency semicircle is associated a film resistance, of the order of tens ohms ($R_f = 13.4\,\Omega$ at 1 C and $R_{f1} = 17.4\,\Omega$ at C/10). This probably identifies the resistance of a thin film on the Sn surface which is native or at least chemically produced as soon as the cells are assembled. The second, medium-high frequency semicircle, that can be resolved only for electrodes cycled at low current rates, is attributed to a porous thick film which, very likely, is that formed as consequence of the quoted decomposition process associated with the 1.5 V not reproducible anomalous plateau. The resistance of this film, R_{f2}, is high, i.e. of the order of 300 Ω, this suggesting that the film is quite thick in its initial stage.

The constant-phase elements (CPE) for the two electrodes, Q_f and Q_{fl}, are characterized by similar values of the factor Y_0 and of the fractional exponent n, i.e. both of the order of 10^{-4} mho and 0.7, respectively (see Tables 1 and 2, cycle 1). Here the complex impedance Z^* as function of the frequency ω is represented by the equation $Z^*(\omega) = Y_0{}^{-1}(j\omega)^{-n}$ [11,12], when $n = 1$ the CPE becomes a pure capacitor with $Y_0 = C$. The high values of Y_0 and the relatively low values of n are justified considering the roughness of the electrodes associated with their pronounced pillar morphology, see Fig. 1, this suggesting that the value of the active area is effectively much higher than that of the geometrical one (0.785 cm^{-2}).

Finally, the medium-low frequency semicircle, which is attributed to the kinetics of the electrochemical process (1), gives a value of charge transfer resistance, R_{ct}, which is rather high in the fully charged state, i.e., 972 Ω at 1 C and 720 Ω at C/10.

To be noticed that a remarkable decrease, i.e. of about one order of magnitude, is observed for the resistance of the anomalous film R_{f2}, after 10 discharge cycles at C/10 (compare Cycle 1 with Cycle 10 in Table 2). This suggests that the electrode may be "cleaned" by current flow, this in turn promoting disintegration or even, dissolution of the film. Little changes are observed in the other parameters.

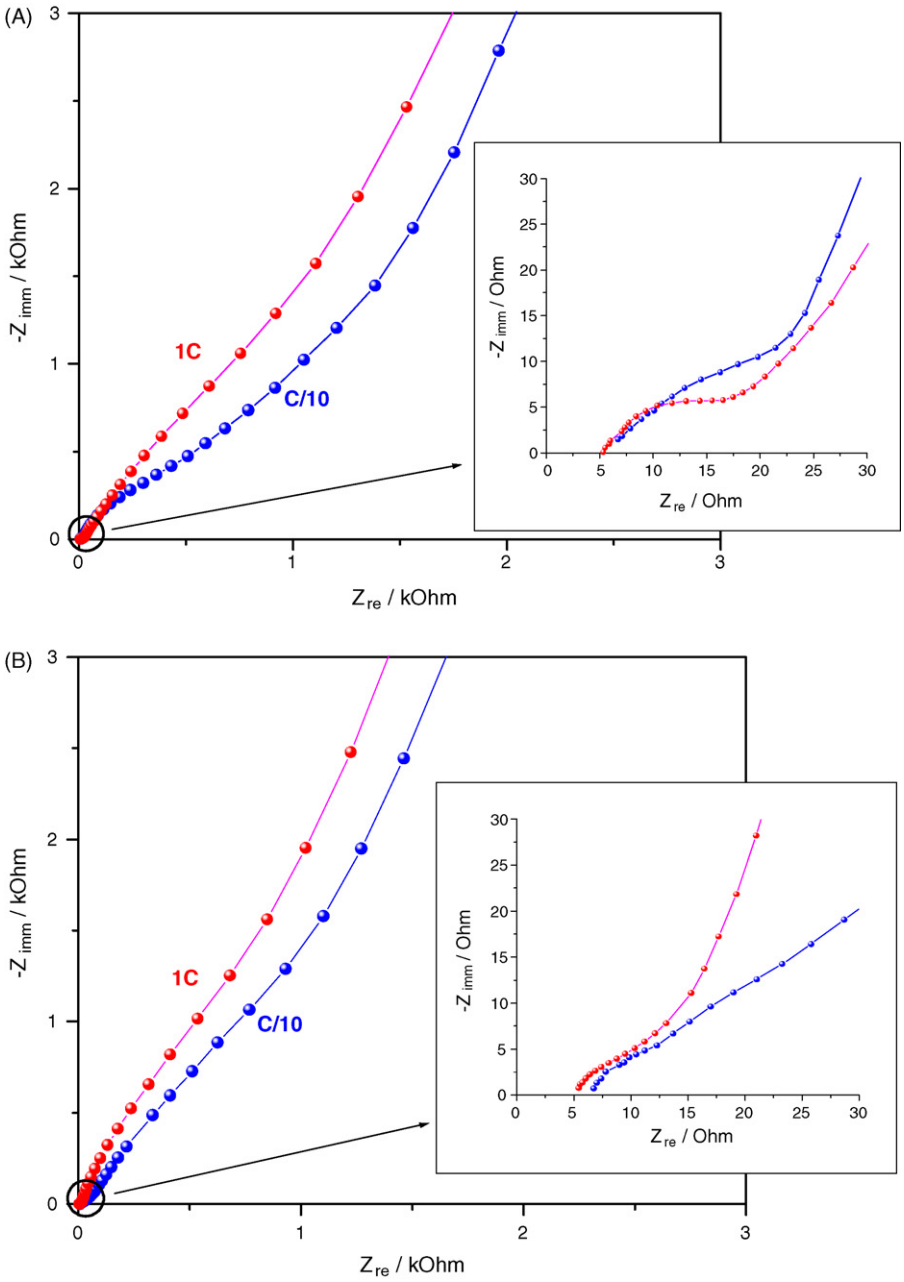

Fig. 7. Impedance response of Sn/EC:DMC 1:1 $LiPF_6$/Li cells cycled at C/10 rate and at 1 C rate after the first cycle (A) and after the tenth discharge charge cycles (B). Frequency range: 100 kHz to 0.005 Hz. Room temperature. The insets enlarge the response of the high frequency region.

These results clearly show that the response of a tin electrode may be greatly influenced by its interfacial status and indirectly, by the modus of its operational conditions. To investigate the practical reflections of this important aspect, we have assembled two complete lithium-ion cells by using electrodeposited Sn as the anode and a $LiNi_{0.5}Mn_{1.5}O_4$ as the cathode [6]. One of the two cells was cycled at 1 C rate versus the cathode, this corresponding to a C/3 rate versus the anode. The other

Table 1
Impedance parameters associated to a Sn/EC:DMC 1:1 $LiPF_6$/Li cell cycled at 1C rate

	R_e	R_f	Q_f Y_0	n	R_{ct}	Q_{ct} Y_0	n	Q_g Y_0	n
Cycle 1	5.4	13.4	1.1×10^{-4}	0.74	972	2.7×10^{-3}	0.68	2.9×10^{-3}	0.79
Cycle 10	5.5	7.6	4.1×10^{-4}	0.83	450	3.9×10^{-3}	0.90	2.2×10^{-3}	0.81

R_e electrolyte ionic resistance, Q_f film CPE, R_f film resistance, Q_{ct} double layer CPE, R_{ct} charge transference resistance, Y_0 factor, n fractional exponent, Q_g cell geometric CPE.

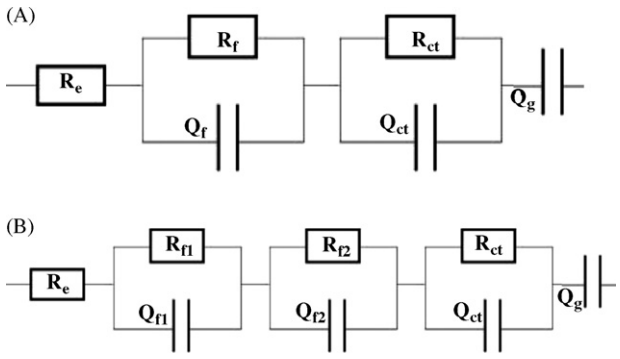

Fig. 8. The general equivalent circuits used to represent the Sn/EC:DMC 1:1 $LiPF_6$/Li electrochemical cells cycled at C/10 rate (A) and at 1 C rate (B). R_e electrolyte ionic resistance, Q_f film CPE, R_f film resistance, Q_{ct} double layer CPE, R_{ct} charge transference resistance, Q_g cell geometric CPE.

cell was first rapidly cycled at 3 C rate versus the cathode (1 C rate versus the anode) for two cycles and subsequently under the same conditions of the first cell, i.e. at 1 C rate versus the cathode.

Fig. 10A shows the response of the first cell in terms of capacity (referred to the cathode) versus cycle number. A net capacity decay is observed and this is a clear evidence of the dramatic effect of the Sn surface film whose formation is favoured by the low cycling rate. Quite different is the response of the second cell, still evaluated in terms of capacity (referred to the cathode) versus cycle number, see Fig. 10B. In this case, due to the control of the film formation in the course of the initial, high rate step, the cell cycles with an optimized capacity retention. This is consistent with the impedance spectroscopy analysis which, in agreement with the literature data [1,2], confirms that cycling at low current regimes gives rise to a complex, thick film formation on the Sn electrode surface. However, the impedance analysis also shows that the film may be consumed

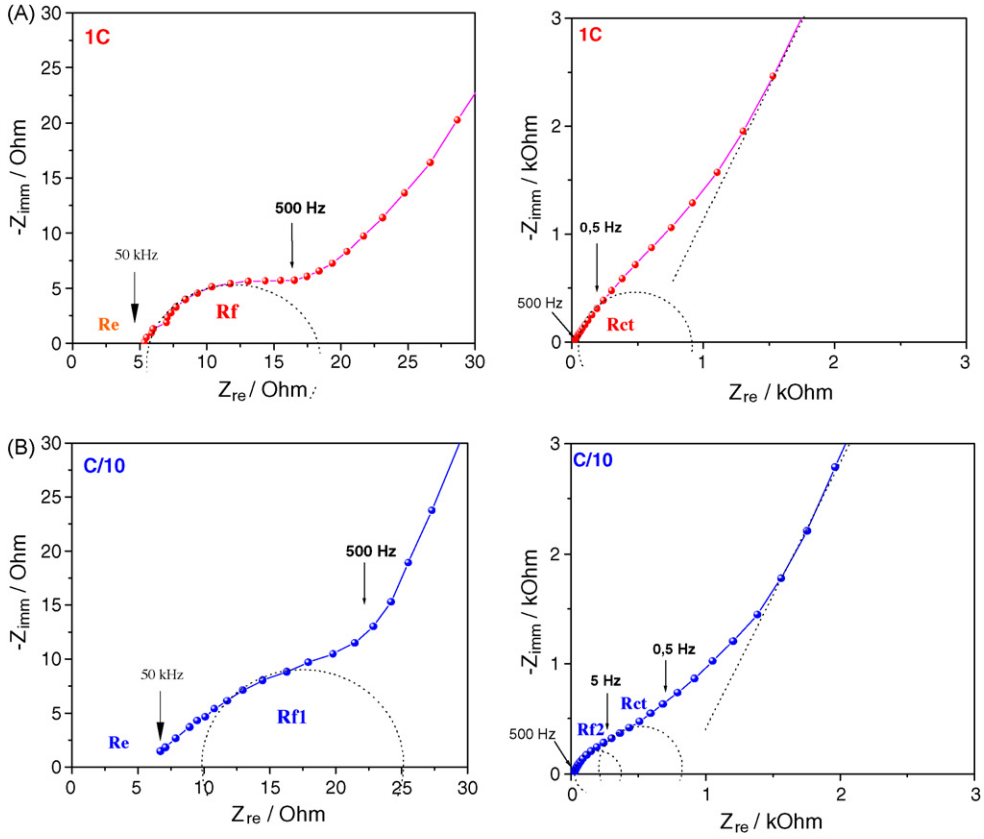

Fig. 9. The overlapping of the impedance responses after the first cycle and an approximate representation of the correspondent circuital elements for the cells cycled at 1 C (A) and at C/10 (B). R_e electrolyte ionic resistance, R_f film resistance, R_{ct} charge transference resistance.

Table 2
Impedance parameters associated to a Sn/EC:DMC 1:1 $LiPF_6$/Li cell cycled at C/10 rate

	R_e	R_{f1}	Q_{f1}		R_{f2}	Q_{f2}		R_{ct}	Q_{ct}		Q_g	
			Y_0	n		Y_0	n		Y_0	n	Y_0	n
Cycle 1	6.1	17.4	6.9×10^{-5}	0.70	300	1.5×10^{-4}	0.88	720	6×10^{-4}	0.82	8.6×10^{-4}	0.78
Cycle 10	6	15.7	4.9×10^{-4}	0.58	49	8×10^{-4}	0.62	915	8.8×10^{-4}	0.76	1.8×10^{-3}	0.83

R_e electrolyte ionic resistance, Q_{f1} first film CPE, R_{f1} first film resistance, Q_{f2} second film CPE, R_{f2} second film resistance, Q_{ct} double layer CPE, R_{ct} charge transference resistance, Y_0 factor, n fractional exponent, Q_g cell geometric CPE.

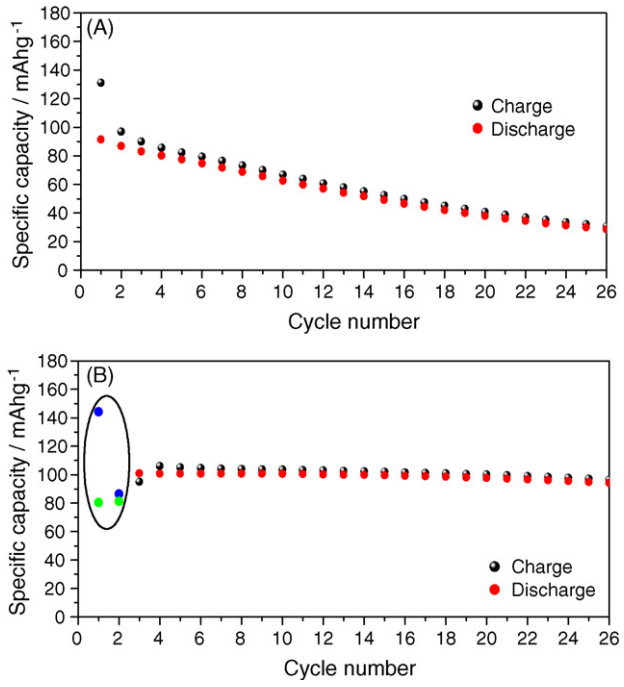

Fig. 10. Specific capacity vs. cycle number of a Sn/EC:DMC 1:1 $LiPF_6/LiNi_{0.5}Mn_{1.5}O_4$ lithium-ion cell cycled under different conditions, i.e., at 1 C rate vs. the cathode (C/3 rate vs. the anode) (A) and first at 3 C rate vs. the cathode (1 C rate vs. the anode) for two cycles and subsequently at 1 C rate vs. the cathode (B). Charge–discharge current density: 0.2 A cm^{-2} g^{-1} vs. $LiNi_{0.5}Mn_{1.5}O_4$, about 1 C rate.

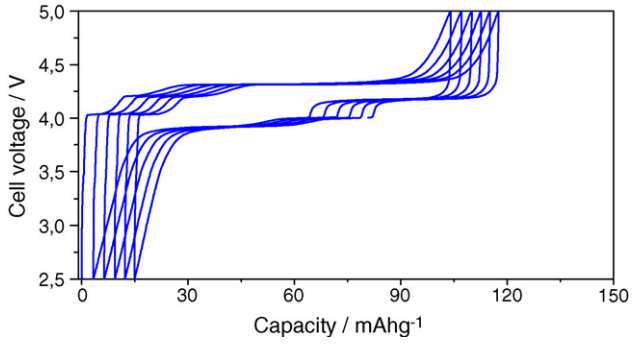

Fig. 11. Voltage vs. specific capacity profiles after the first two cycles of a Sn/EC:DMC 1:1 $LiPF_6/LiNi_{0.5}Mn_{1.5}O_4$ lithium-ion cell cycled at 3 C rate vs. the cathode (1 C rate vs. the anode) for two cycles and subsequently at 1 C rate vs. the cathode (0.2 A cm^{-2} g^{-1}).

by particles detachment or by dissolution induced by current flow.

Fig. 11 reports the voltage versus capacity profile of the cell cycled under optimized conditions (see Fig. 10B). The curve results as the combination of the expected profile associated with the Li–Sn alloy formation [5] and that related to the $LiNi_{0.5}Mn_{1.5}O_4$ cathode [6].

We may then conclude that the formation of the surface film does compromise the performance of electrodes which expose the Sn surface to the electrolyte, and thus, that the control of the experimental cycling conditions may play a key role in determining the response of lithium-ion batteries using conventional tin-based anodes.

Acknowledgements

This work has been carried out with the financial support of the European Network of Excellence ALISTORE and of the Italian Ministry of University and Research under a PRIN 2005 project. The authors thank Dr A. Martinelli, University of Rome "La Sapienza", for assistance and discussions with IR measurements. We are also grateful to Professor F. Croce University of Chieti "d'Annunzio" and Professor B. Scrosati, University of Rome "La Sapienza", for their helpful suggestions of this paper.

References

[1] S.D. Beattie, T. Hatchard, A. Bonakdarpour, K.C. Hewitt, J.R. Dahn, J. Electrochem. Soc. 150 (2003) A701.
[2] L.Y. Beaulieu, S.D. Beattie, T. Hatchard, J.R. Dahn, J. Electrochem. Soc. 150 (2003) A419.
[3] S.D. Beattie, J.R. Dahn, J. Electrochem. Soc. 150 (2003) 894.
[4] A.S. Aricò, P. Bruce, B. Scrosati, J.M. Tarascon, W. Van Schalkwijk, Nature Mater. 4 (2005) 366.
[5] J. Hassoun, S. Panero, B. Scrosati, Int. J. Electrochem. Sci. 1 (2006) 110–121.
[6] P. Reale, S. Panero, B. Scrosati, J. Electrochem. Soc. 152 (10) (2005) 1949–1954.
[7] J. Hassoun, S. Panero, B. Scrosati, J. Power Sources 160 (2006) 1336–1341.
[8] S. Geniès, R. Yazami, J. Garden, J.C. Frison, Synth. Met. 93 (1998) 77–82.
[9] D. Aurbach, A. Zaban, Y. Gofer, Y.E. Ely, I. Weissman, O. Chusid, O. Abramson, J. Power Sources 54 (1995) 76–84.
[10] D. Aurbach, J Power Sources 89 (2000) 206–218.
[11] B.A. Boukamp, Solid State Ionics 18 (1986) 136.
[12] B.A. Boukamp, Solid State Ionics 20 (1986) 31.